CALIBRATION OF CURVATURE OF FIELD FOR DEPTH FROM FOCUS

G. Blahusch*, W. Eckstein, C. Steger

MVTec Software GmbH, Neherstr. 1, 81675 München, Germany - (blahusch, eckstein, steger)@mvtec.com

Commission III, WG III/5

KEY WORDS: Metrology, Calibration, Depth from Focus, Optical Aberration, Curvature of Fields, Algorithms

ABSTRACT:

A method for accurate depth measurement in depth from focus is presented. With depth from focus the 3D shape of objects can be measured. To do so, an image series with different distances between camera and object is evaluated to extract focused parts. Combining the results of an edge detection filter with the distance information at which the images have been acquired provides a depth image of the object. The focus information is influenced by optical aberrations. Especially the curvature of field leads to a significant error in the depth image. This error can be seen by measuring the depth information of a planar object with depth from focus. The error in the depth image is approximated by fitting a second order surface to the depth image. To overcome the influence of outliers in the depth image a robust least-squares fitting with suppression of outliers is used. The second order surface is then used to correct depth images, which reduces the influence of the curvature of field on the depth data and leads to more accurate 3D measurements.

1. INTRODUCTION

The measurement of spatial geometric parameters of objects needs accurate methods to obtain the 3D shape of the object. There exist different methods to extract the 3D shape of an object. Often structured light, interferometrical techniques, or a stereo setup with two or more cameras are used. However all these methods require a complex and expensive setup. A simple setup uses one camera and applies the well known "depth from focus" (DFF) method to measure the 3D parameters of objects (Nayar, 1992; Nayar, 1994).

The principle of DFF is the use of a lens system with a very short depth of field in combination with the evaluation of an image series, where every image is taken at a different camera-object distance. Therefore, the advantage of DFF is the relatively simple setup. One just needs to take images at different distances to the object. The 3D shape information is then calculated from the image series by determining for every pixel the image in which the pixel is focused best. The result of the evaluation of the image series is a range image with the depth information of the object. This range image can be used to obtain further information about the object, e.g., the measurement of the volume of the object or the calculation of orientation information from the shape of the object. This requires accurate data in the range image. However, up to now the influence of optical aberrations has been neglected in the calculation of the range image. In this paper we propose a method to correct the effects of optical aberrations in order to get a more accurate range information. The proposed method can also be used in other ranging techniques, where depth information is obtained from focus measurements, e.g. in depth from defocus (Chaudhuri, 1998).

2. EXPERIMENTAL SETUP

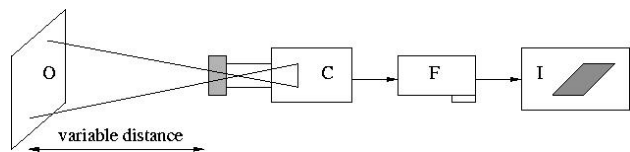A sketch of the experimental setup is shown in Figure 1.

Figure 1: Schematic view of the setup (O: object, C: camera and optics, F: framegrabber, I: image processing)

The camera with the optical system (C) acquires images of the object (O). The distance between the camera and the object is variable. The camera is connected to a framegrabber (F) inside a standard computer. The image processing (I) is done in software on a standard computer. The image processing and the DFF algorithm are implemented in HALCON, the image processing library from MVTec.

The camera is a standard CCD camera with a resolution of 768x578 pixels. The optical system consists of a perspective lens with 16 mm focal length and a depth of field of approximately 0.4 mm. Using a perspective lens system may cause problems in finding point-to-point correspondences between the pixels of the images from different distances. Therefore often a telecentric lens system is used for DFF applications to overcome the problem of perspective distortion (Watanabe, 1995). The aperture of a telecentric lens is positioned directly at its focal point. Hence, only parallel rays are able to pass through this aperture and therefore a parallel projection of the object onto the CCD chip is achieved. In practice, however, true telecentricity can never be obtained.

---

* Corresponding author.

3. OPTICAL ABERRATIONS

3.1 Motivation

To demonstrate the influence of optical aberrations on the range information, we use a planar textured plate. The texture is necessary to get enough edge information for the DFF method. The plate is oriented parallel to the plane of the optical sensor. Examples for images of the plate at different distances are shown in Figure 2 and Figure 3. The part of the plate that is at the focus distance shows sharp edges, while all others parts are blurred. With the variation of the distance the sharp area moves over the surface of the object.
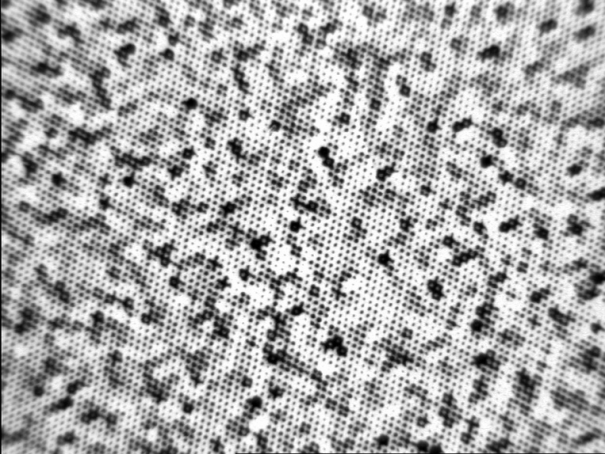
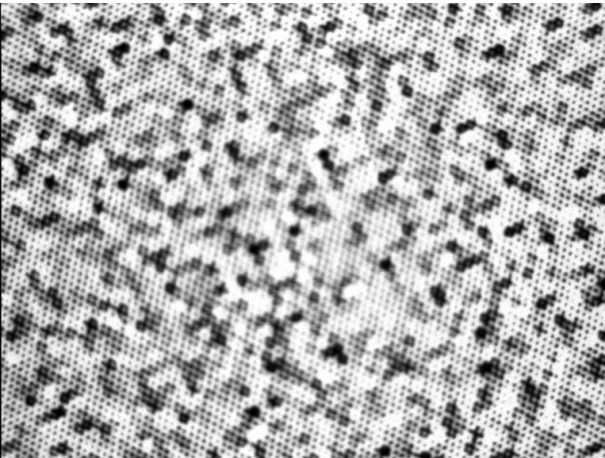Figure 2: Planar plate with the image center in focus

Figure 3: Planar plate with the image border in focus

In Figure 2 mainly the center part of the object is in focus, while border parts are blurred. In contrast, in Figure 3 the center part is blurred, while the border area is sharp. The effect that in an aligned setup even a planar object cannot be imaged completely sharp is an effect of the optical aberrations, in particular the curvature of field.

3.2 Theory of Optical Aberrations

There exist different types of optical aberration. A detailed description of the different types of aberration can be found in (Born, 1998). The main errors caused by aberrations are the following ones. Because of spherical aberration, light rays have different focus points depending on their distance to the optical axis. This kind of aberration causes a noticeable softness of the image. The coma is formed by an asymmetric accumulation of light intensity for off-axis points. It refers to the situation in which rays from a single point in the focal plane, but passing through opposite sides of the aperture, converge to different points in the image. Coma appears in an image with comet-like extension, affecting the periphery of the field of view. The astigmatism is the separation of the tangential and sagittal focal surface. For example in the case of astigmatism horizontal lines appear in focus and vertical lines out of focus, and vice versa.

The distortion is the reason that straight lines that are off-axis are imaged as curved lines. With distortion the image differs geometrically from the object. The two types of distortion are called barrel and pincushion distortion. For accurate measurements in images it is necessary to correct the effects of distortions. With a suitable calibration, based on a pinhole camera model and the assumption of only radial distortion, this effect can be corrected (Beyer, 1990; Gruen, 2001; Lanser, 1995).

The curvature of field is the curvature of the tangential and sagittal fields. This means that a planar object at right angles to the axis of an optical system does not appear as a planar image. Therefore, one can focus around the center of the field, but the periphery of the field will appear out of focus, or vice versa. This effect is the reason for the different sharp areas of Figure 2 and Figure 3. Figure 4 shows a ray diagram of the geometric representation for this effect.
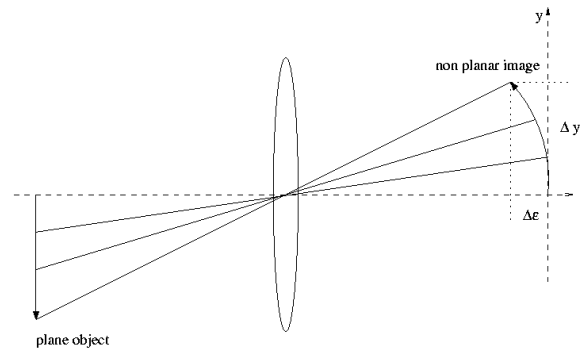
Figure 4: Ray diagram for the curvature of field

A planar object is mapped on a non planar object. The distance $\Delta\varepsilon$ between the planar image and the non planar image depends on the distance Δy from the optical axis. It can be shown that

$$\Delta\varepsilon \propto \Delta y^2 \qquad (1)$$

(Born, 1998). The curvature of field leads to different distances where an object is focused, depending on the distance to the optical axis. Therefore, the accuracy of the depth information in DFF is limited by the curvature of field.

4. DEPTH FROM FOCUS

4.1 Principle

The DFF algorithm calculates depth information from a series of images. For every pixel in the image series, the maximum response of an edge detection filter is calculated. As a result, for every pixel the information in which image it is focused is

returned. To show the result we can construct a completely sharp image of the object. For this we take for every pixel the gray value from the image where it is focused. Figure 5 shows the completely sharp image for the image series of Figure 2 and Figure 3.
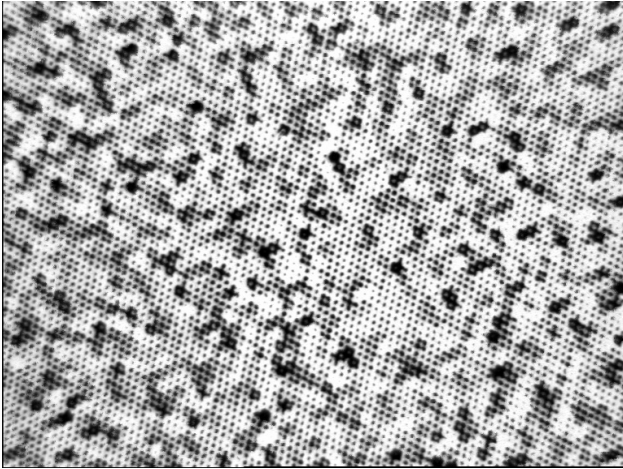

Figure 5: Constructed completely sharp image

4.2 Depth Information

Another information that is available is the distance at which the image was captured. This can be combined with the information for the completely sharp image. The result is an image representing the depth information of the object. Different depths are represented by different gray values. The resulting depth image for the image series of Figure 2 and Figure 3 is shown in a pseudo 3D-plot in Figure 6.
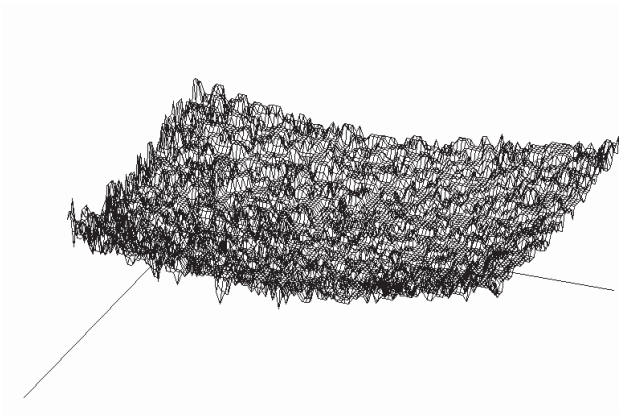

Figure 6: Depth image

Different depths are displayed as different heights in Figure 6. At the border of the image we have a different depth compared to the center of the image. For a planar object perpendicular to the optical axis we would expect a constant depth. The different depths are the result of the curvature of field.

4.3 Depth correction

When measuring a planar object vertical to the optical axis the resulting depth image is not a simple plane. It is a combination of a plane with a curved surface. The distance between the plane and the curved surface, caused by the curvature of field, can be used for a correction of the depth.

Using Figure 6 as an error image includes, albeit small, errors from noise and other perturbations. Even though the object has a smooth surface, the depth image is not perfectly smooth. To achieve a more robust error image, it is useful to approximate the error image by a curved surface.

A suitable approach is to fit a second order surface $\Delta\varepsilon(x,y)$:

$$\Delta\varepsilon(x, y) = ax^2 + by^2 + cxy + dx + ey + f, \qquad (2)$$

where x and y are the pixel position in the error image and a to f are the fitting parameters. The parameters a, b, and c are responsible for the curvature, the parameters d and e are the linear part in the x- and y- direction, and f is a constant offset.

The fitting of the surface can be done with a least squares method by minimizing the distance between the surface and the error image. This means that the following function needs to be minimized with respect to the parameters a, b, c, d, e, and f:

$$\varepsilon = \sum_{x,y} e_{x,y}^2 = \sum_{x,y} (\Delta\varepsilon(x, y) - I(x, y))^2 \qquad (3)$$

ε is the sum over all pixels (x,y) of the squared distances $e_{x,y}$ between the curved surface $\Delta\varepsilon$ and the measured depth image I. The function ε is minimized if $D\varepsilon = 0$, where D are the partial derivatives of ε with respect to the parameters a to f (Haralick, 1992).This leads to an overdetermined set of linear equations of the form Ax = b, which can be solved by standard numerical methods, e.g., the singular value decomposition (SVD).

The standard least squares fitting yields good results as long as there are no gross outliers in the depth image. Since the calculated depth image will usually contain outliers, robust least squares fitting procedures are necessary to suppress outliers in the fitting procedure. To achieve this, the least squares function is replaced by a new function for the distance between the curved surface and the error image.

$$\varepsilon = \sum_{x,y} \rho(e_{x,y}) \qquad (4)$$

The new function ρ increases slower than the quadratic function of the standard least squares minimization. Minimizing the new function is again done by setting the partial derivatives to zero. The result can be written again as a least squares problem with a weighting function:

$$\varepsilon_k = \sum_{x,y} w(e_{x,y}^{(k-1)}) e_{x,y}^2 \qquad (5)$$

The weighting function w is a function of the distance e_{xy}. The calculation of the parameters is now done in an iterative process. In every step the weighting function w is evaluated

from the distances $e_{x,y}$ of the preceding step (k-1). The equation is solved, and a new set of parameters is calculated. This is done until the resulting error is smaller than a upper limit or a fixed number of iterations is reached.

For the weighting function different approaches can be used. The approach of Tukey uses the following weighting function (Mosteller, 1977):

$$w(e) = \begin{cases} \left[1 - (e/a)^2\right]^2 & : \quad |e| \le a \\ 0 & : \quad |e| > a \end{cases} \quad (6)$$

The clipping factor a controls the damping of outliers. It specifies, which distances are treated as outliers. Distances e greater than the clipping factor are completely ignored.

The approach of Huber treats outliers not as restrictive as Tukey (Huber, 1981). With the weighting function

$$w(e) = \begin{cases} 1 & : \quad |e| \le a \\ a/|e| & : \quad |e| > a \end{cases} \quad (7)$$

outliers are not completely eliminated, but their contribution is damped. Outliers contribute only linearly instead of quadratically to the total error.

From equations (5) and (7), using a clipping factor of twice the standard deviation, a more robust error image is obtained by evaluation of the curved surface at every pixel position in the error image. The calculated error image is shown in Figure 7.
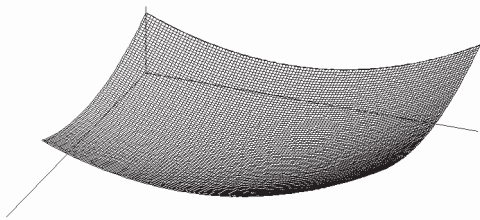

Figure 7: Calculated error image from the measured depth image

For further measurements the depth at the position (x,y) can now be corrected with the value $\Delta\varepsilon(x,y)$.

5. RESULTS

We have tested the proposed method by applying it to a variety of objects with different types of shapes. Figure 8 shows the depth image of a plane, which is not perpendicular to the optical axis.
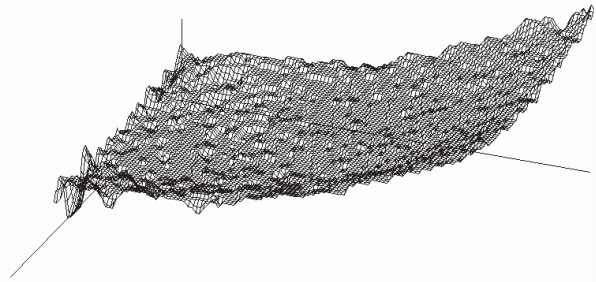

Figure 8: Depth image of a plane

The depth image of the plane shows the plane with an overlay from the curvature of field. The distortion generates a curved surface in contrast to a planar surface as expected. The resulting depth image after the correction with the error image from Figure 7 is shown in Figure 9. As expected, the depth image doesn't show a significant curvature anymore.
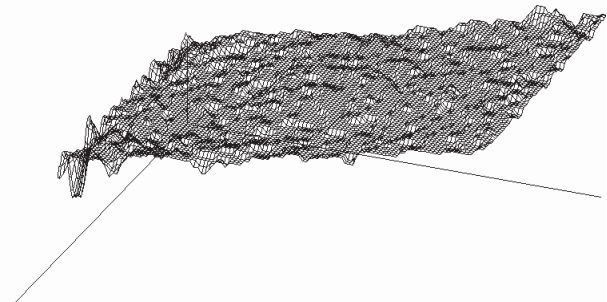

Figure 9: Depth image of a plane after the correction

Another example is shown in Figure 10, where the depth image of a cylinder is displayed.
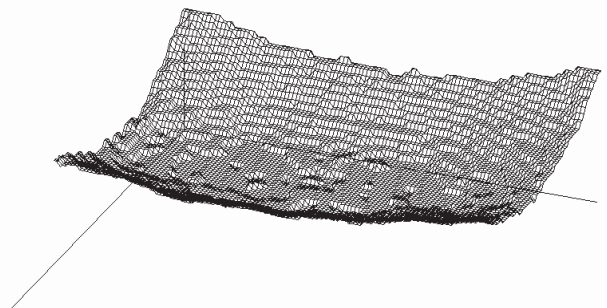

Figure 10: Depth image of a cylinder

The deformation at the border leads to significant errors in the depth data. In contrast Figure 11 shows the depth image after the correction with the error image of Figure 7.
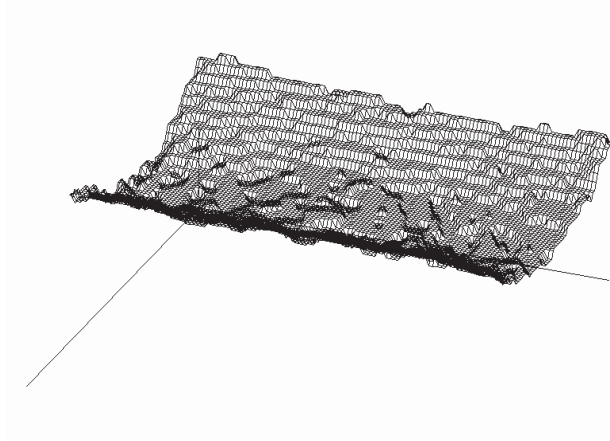

Figure 11: Depth image of a cylinder after the correction

The depth image shows the shape of a cylinder as expected.

6. CONCLUSIONS

Based on the DFF algorithm, we have developed a method to correct range errors caused by optical aberrations. An error image is calculated from an image series of a plane that is oriented perpendicular to the optical axis. The curvature of field is the type of aberration that is responsible for depth errors. The curvature of field is determined by fitting a second order surface to the error image using a robust least-squares fit with outlier suppression. The depth information to be measured can then be corrected with this second order surface, leading to a significantly more accurate depth information.

REFERENCES

Beyer H. A., 1990. Linejitter and geometric calibration of CCD-cameras. *ISPRS Journal of Photogrammetry and Remote Sensing*, 45, pp. 17–32.

Born M., Wolf E., 1998. *Principles of Optics*. Sixth Edition, Cambridge University Press, pp. 203–218.

Chaudhuri S., Rajagopalan A. N., 1998. *Depth From Defocus: A Real Aperture Imaging Approach*. Springer-Verlag, Berlin.

Gruen A., Huang T. S., 2001, *Calibration and Orientation of Cameras in Computer Vision*. Springer-Verlag, Berlin.

Haralick R. M., Shapiro L. G, 1992, *Computer and Robot Vision*, volumne I, Addison-Weseley Publishing Company, Reading, MA, pp. 73-80.

Huber, P. J., 1981. *Robust Statistics*. John Wiley & Sons, NY.

Lanser S., Zierl C., Beutlhauser R., 1995, Multibildkalibrierung einer CCD-Kamera. *Mustererkennung*, *Informatik aktuell*, Springer-Verlag, Berlin, pp. 481–491.

Nayar, S. K., 1992. Shape from Focus System. *Proc. IEEE Conf. on Computer Vision and Pattern Recognition*, Champaign, Ill., pp. 302-308.

Nayar, S. K., 1994. Shape from Focus. *IEEE Trans. on Pattern Analysis and Machine Intelligence*, 16(8), pp. 824-830.

Mosteller F., Tukey M., 1977. *Data Analysis and Regression*. Addison-Weseley Publishing Company, Reading, MA.

M. Watanabe 1995. Telecentric Optics for Constant-Magnification Imaging. In: *Technical Report CUCS-026-95*, Dept. of Computer Science, Columbia University, New York, NY, USA.